JOURNAL OF VIROLOGY, Nov. 2006, p. 11082–11093 Vol. 80, No. 22
0022-538X/06/$08.00+0 doi:10.1128/JVI.01307-06

Persistent Hepatitis C Virus Infection In Vitro: Coevolution of Virus and Host▽†

Jin Zhong,[1] Pablo Gastaminza,[1] Josan Chung,[1] Zania Stamataki,[1] Masanori Isogawa,[2] Guofeng Cheng,[2] Jane A. McKeating,[2] and Francis V. Chisari[1]*

Department of Molecular and Experimental Medicine, The Scripps Research Institute, La Jolla, California 92037,[1] *and Division of Immunity and Infection, Institute of Biomedical Research, Medical School, University of Birmingham, Birmingham B15 2TT, United Kingdom*[2]

Received 21 June 2006/Accepted 29 August 2006

The virological and cellular consequences of persistent hepatitis C virus (HCV) infection have been elusive due to the absence of the requisite experimental systems. Here, we report the establishment and the characteristics of persistent in vitro infection of human hepatoma-derived cells by a recently described HCV genotype 2a infectious molecular clone. Persistent in vitro infection was characterized by the selection of viral variants that displayed accelerated expansion kinetics, higher peak titers, and increased buoyant densities. Sequencing analysis revealed the selection of a single adaptive mutation in the HCV E2 envelope protein that was largely responsible for the variant phenotype. In parallel, as the virus became more aggressive, cells that were resistant to infection emerged, displaying escape mechanisms operative at the level of viral entry, HCV RNA replication, or both. Collectively, these results reveal the existence of coevolutionary events during persistent HCV infection that favor survival of both virus and host.

The hepatitis C virus (HCV) is a hepatotropic, positive-stranded RNA virus that causes acute and chronic hepatitis. Because most infections become persistent, HCV chronically infects more than 170 million people worldwide, many of whom will develop liver cirrhosis and hepatocellular carcinoma (15). HCV is thought to be noncytopathic in vivo, and the pathogenesis of the associated hepatitis is assumed to reflect destruction of HCV infected cells by cytotoxic $CD8^+$ T cells (9).

HCV is the sole member of the genus *Hepacivirus* in the *Flaviviridae* family. Its 9.6-kb RNA genome encodes a long open reading frame that is co- and posttranslationally cleaved by cellular and viral proteases into structural (core, E1, E2, and p7) and nonstructural (NS2, NS3, NS4A, NS4B, NS5A, and NS5B) proteins (2). The viral life cycle and the host-virus interactions that determine the outcome of HCV infection have been difficult to study due to the absence of a tissue culture model of HCV infection. Recently, several groups (16, 20, 25, 29, 31) have developed cell culture models of HCV infection that release HCV particles that are infectious for human hepatoma-derived cell lines. The most robust of these in vitro infections are based on the extraordinary replicative capacity of the genotype 2a JFH-1 strain of HCV, which replicates efficiently in vitro without requiring adaptive mutations (14). Importantly, cell culture-derived JFH-1 and a chimeric virus expressing the structural region of the related J6 strain of HCV and the nonstructural region of JFH-1 are infectious for chimpanzees and uPA-SCID mice reconstituted with human hepatocytes (17, 25).

At present, the cell culture system has been used primarily to study the early steps of HCV infection. For example, we and others (16, 31) have reported that primary HCV infection can be inhibited by blocking the interaction between the HCV E2 glycoprotein and the cellular protein CD81, an important co-receptor for HCV entry (3, 13, 18, 30). In the current study, we used the cell culture system to elucidate the virological and cellular consequences of persistent HCV infection. Here, we demonstrate that HCV can establish persistent infection in vitro for at least 6 months and that it can induce cytopathic effects when expressed at high levels, which lead to the selection of viral and host variants that favor the survival of both. The viral evasion and host survival mechanisms illustrated in this report may provide insights into the pathophysiology of chronic HCV infection and, possibly, other persistent RNA virus infections as well.

MATERIALS AND METHODS

Cell culture, molecular cloning, in vitro transcription, and HCV RNA transfection. The cell culture condition and protocols for in vitro transcription and HCV RNA electroporation have been described previously (31). Individual viral mutations were introduced into the pJFH-1 plasmid (25) by two-step recombinant PCR using primers containing the mutation, followed by restriction digestion and ligation (protocols are available upon request). All constructs were verified by DNA sequencing.

RNA analysis, indirect immunofluorescence, and titration of infectious HCV. RNA Isolation and quantitative reverse transcription-PCR (RT-QPCR) analysis of intracellular HCV RNA were performed as previously described (31). The CD81 mRNA levels were measured by RT-QPCR with the primers 5′-CACTG ACTGCTTTGACCACC-3′ and 5′-CACCATGCTCAGGATCATCTC-3′ and normalized to cellular GAPDH (glyceraldehyde-3-phosphate dehydrogenase) levels. Intracellular staining was performed as previously described, using polyclonal anti-NS5A rabbit antibody MS5 (31). Titration assays were performed as previously described using Huh-7.5.1 cells (31).

HCV infection kinetics assay. Eighty thousand Huh-7.5.1 cells were seeded in 12-well plates overnight and then inoculated with HCV at the multiplicity of

* Corresponding author. Mailing address: Department of Molecular and Experimental Medicine, SBR-10, The Scripps Research Institute, 10550 North Torrey Pines Road, La Jolla, California 92037. Phone: (858) 784-8228. Fax: (858) 784-2160. E-mail: fchisari@scripps.edu.

† Supplemental material for this article may be found at http://jvi.asm.org/.

▽ Published ahead of print on 6 September 2006.

infection (MOI) indicated in the figure legends. The infected cells reached confluence on day 4 postinfection and were then split at a ratio of 1:3 into 12-well plates (harvested on day 6), 6-well plates (harvested on day 8 or 9), and T25 flasks (harvested on day 10 or at later time points). No split was necessary after day 10 due to cytopathic effects of the infection. Culture supernatants were collected at the indicated time points, and infectivity titers were determined by titrating on Huh-7.5.1 cells.

Sedimentation equilibrium gradient analysis. Gradients were formed by overlaying 700 μl of 20%, 30%, 40%, 50%, and 60% sucrose solutions in TNE buffer (10 mM Tris-HCl [pH 8], 150 mM NaCl, 2 mM EDTA). Approximately 250 to 500 μl of viral supernatants with infectivity titers of 10^4 focus-forming units (FFU)/ml were overlaid on the gradients. Equilibrium was reached by ultracentrifugation (SW41Ti rotor; Beckman Instruments, Palo Alto, CA) for 16 h at 120,000 × *g* at 4°C. Fifteen fractions of 250 μl were collected from the top and analyzed for virus infectivity titers as described above. The density of each fraction was determined by measuring the mass of 100-μl aliquots in each sample.

HCV RNA genome sequencing. HCV RNA was isolated from 0.3 ml of viral supernatants with infectivity titers between 10^3 and 10^5 FFU/ml by the guanidine thiocyanate method (27) and then used as a template to generate cDNA in a reverse transcription reaction, followed by two rounds of nested PCR. The protocols for reverse transcription and nested PCR and the primer sequences were provided by J. Bukh (unpublished data).

Blockade of HCV infection by CD81 antibody. Ten thousand Huh-7.5.1 cells were pretreated with 0, 0.1, 0.25, 1, 2.5, and 25 μg/ml of CD81 antibody (clone 5A6; Santa Cruz Biotechnology, Santa Cruz, CA) for 1 h and then infected with ~50 focus-forming units of the wild-type or G451R mutant viruses for 5 h in a 96-well plate. The viruses were removed, and the cells were washed with phosphate-buffered saline and then supplemented with complete medium. The efficiency of the infection was monitored 3 days later by quantitating the number of HCV-positive foci by immunofluorescence as described above.

Isolation of HCV-negative cells by serial dilution. Persistently infected R1, R2, and Huh-7 cells, which are designated Huh-7/scr cells in this report, were serially diluted and plated in 96-well plates. The smallest number of seeded cells that can survive in one well of a 96-well plate is 15 to 150. After 2 to 3 weeks of culture, wells with the lowest seeding densities were screened for the presence of infectious HCV in the culture supernatants by the titration assay. The cells with HCV-negative supernatants were expanded, examined for HCV NS5A protein by immunofluorescent microscopy, and confirmed to be HCV RNA negative by RT-QPCR.

CD81 transfection. Plasmid pEE6-hCD81, which expresses human CD81 (12), was transfected into R1, R2, and R3 cells by using Lipofectamine 2000 (Invitrogen, Carlsbad, CA), following the manufacturer's protocol. The cells were seeded in a 6-well plate overnight and were 80 to 90% confluent at the time of transfection. Following transfection, the cells were incubated at 37°C for 18 h and then plated in a 12-well plate (7×10^4 cells per well) and a T25 flask (7×10^5 cells per flask). On day 2 posttransfection, the cells in the T25 flask were collected for CD81 cell surface staining and fluorescence-activated cell sorter (FACS) analysis. At the same time, the cells in the 12-well plate were inoculated with HCV at an MOI of 0.1. The cells were harvested for RNA extraction on day 3 postinfection and analyzed by RT-QPCR for intracellular-HCV-RNA levels.

Flow cytometric analysis of CD81 and SR-BI expression on the cell surface. Approximately 0.3 to 1×10^6 cells were resuspended in 100 μl of staining buffer (1% fetal calf serum–phosphate-buffered saline) and incubated for 1 h on ice with a monoclonal mouse anti-human CD81 antibody (Serotec, Raleigh, NC) or a polyclonal rabbit anti-SR-BI antibody (Novus Biologicals, Littleton, CO) at a 1:100 dilution. After being washed, the cells were incubated in 100 μl of staining buffer for 30 min on ice with phycoerythrin-conjugated anti-mouse immunoglobulin G1 (BD/Pharmingen, San Diego, CA) or anti-rabbit immunoglobulin G (Santa Cruz Biotechnology) at a 1:200 dilution. Cells stained with the respective secondary antibody alone served as negative controls. FACS analysis was performed using the FACSArray Bioanalyzer system (BD Bioscience, San Jose, CA).

HCVpp genesis and infection. HCV pseudotyped retroviral particles (HCVpp) were generated as previously described (13). Briefly, using Lipofectamine, 293T cells were cotransfected with the envelope-deficient human immunodeficiency virus genome pNL4-3.Luc.R-.E- and a plasmid expressing any of the following viral glycoproteins: HCV strain H (genotype 1a), H77 (1a), OH8 (1b), or Con1 (1b); murine leukemia virus (MLV) env; or an empty vector (mock). The medium was replaced with Dulbecco's modified Eagle's medium with 3% fetal bovine serum after 6 h. Supernatants were collected after 48 h and clarified by centrifugation. For infection experiments, supernatants were diluted in Dulbecco's modified Eagle's medium with 3% fetal bovine serum and incubated with cells for 7 h prior to removal and incubation for a further 72 h. Cells were lysed with 40 μl cell culture lysis reagent (Promega, Madison, WI), and infection was measured by quantifying the expression of the luciferase reporter using 50Jl luciferase substrate (Promega) and a Centro LB960 luminometer (Berthold Technologies, Bad Wildbad, Germany).

HCV replicon RNA transfection. One microgram of in vitro-transcribed HCV genotype 1b subgenomic replicon RNA (S1179I) containing a neo marker (7) was electroporated into R1, R2, and R3 cells and their parental Huh-7.5.1 and Huh-7/scr cells, following the electroporation protocol as previously described (31). After electroporation, one-third of the cells were plated in a 10-cm dish. G418 (300 μg/ml) was added 1 day after transfection and was refreshed every 4 to 5 days. G418-resistant colonies were stained with crystal violet 3 weeks after transfection.

RESULTS

Persistent HCV infection in cell culture. To determine whether JFH-1 virus can establish a persistent infection in cell culture, we electroporated JFH-1 genomic RNA into Huh-7/scr and Huh-7.5.1 cells and cultured the transfected cells for up to 6 months. At the indicated time points (normally when the cells were nearly confluent and ready to split), the culture supernatants were assessed for infectious virus, the intracellular-HCV-RNA levels, and the frequency of viral-antigen-NS5A-positive cells. In two independent experiments transfecting Huh-7.5.1 cells (denoted Exp 1 and Exp 2) (Fig. 1A and B), intracellular-HCV-RNA levels decreased significantly during the first few days following transfection and then rebounded, reaching maximal levels (~2×10^7 genome equivalents [GE] per μg cellular RNA) by day 18 posttransfection. Similarly, the levels of infectious extracellular virus reached a peak (10^4 to 10^5 FFU per ml) by day 18 posttransfection, when the majority of cells in the culture expressed NS5A. Interestingly, as illustrated in Fig. S1 in the supplemental material, cell growth rate was greatly reduced and many cells became rounded and floated in the culture medium by day 18 posttransfection, when levels of HCV RNA, antigen, and secreted infectious virus were maximal. The cytopathic effects lasted approximately 2 weeks, after which the cells recovered. Unexpectedly, following the recovery of the levels of intracellular HCV RNA, those of extracellular infectious virus and NS5A-positive cells declined and fluctuated during the following 6 months, indicating the establishment of a dynamic persistent infection. During this period of persistent infection, the cells were cytologically normal although occasionally very minor cytopathic effects were observed.

Transfection of JFH-1 genomic RNA into Huh-7/scr cells (denoted Exp 3) (Fig. 1C) showed similar infection kinetics, although the initial expansion was delayed and the amount of secreted infectious virus reduced, reaching a peak of 6×10^3 FFU/ml by day 26 posttransfection. In contrast to what was found for Huh-7.5.1 cells, minimal cytopathic effects were observed in Huh-7 cells at the peak of JFH-1 infection (Fig. S1 in the supplemental material). Nonetheless, as with Huh-7.5.1 cells, the amounts of secreted infectious virus and intracellular HCV RNA and the frequency of NS5A-positive cells decreased significantly after reaching peak levels and fluctuated widely thereafter for at least 6 months (Fig. 1C).

In subsequent experiments, we established persistent HCV infections in Huh-7.5.1 (Fig. S2 in the supplemental material) and Huh-7/scr (not shown) cells by inoculating them with virus produced in the transfection experiments described above. These persistent infections displayed the same characteristics

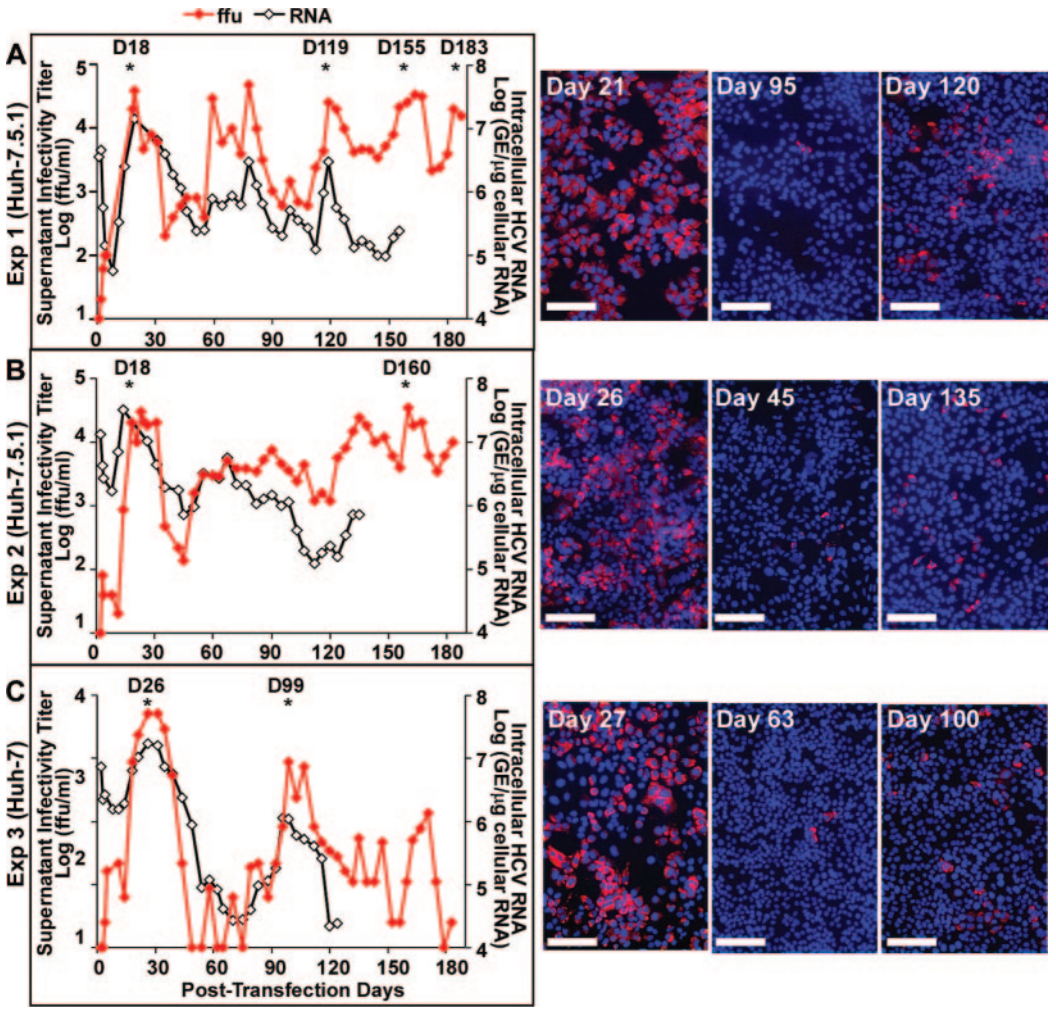

FIG. 1. Persistent HCV infection in Huh-7.5.1 and Huh-7/scr cells. Cells were transfected with 10 μg JFH-1 RNA and maintained in culture for 6 months. Infectious-viral titers in the culture supernatants (red diamonds, left *y* axis) and intracellular-HCV-RNA levels (black open diamonds, right *y* axis) were measured by the titration assay and RT-QPCR and are expressed as numbers of FFU/ml and GE/μg cellular RNA, respectively. NS5A immunostaining of transfected cells at the selected time points is shown in the right-hand panels. NS5A is red (Alexa 555), and nuclei are blue (Hoechst). The scale bar represents 100 μM. The asterisks represent the time points (days 18, 119, 155, and 183 of Exp 1, days 18 and 160 of Exp 2, and days 26 and 99 of Exp 3) at which we collected viruses for the infection kinetics assays whose results are shown in Fig. 2.

as those described above, indicating that persistence is independent of the process used to initiate the infection.

Collectively, these results indicate that HCV can persistently infect Huh-7.5.1 and Huh-7/scr cells in vitro, HCV infects the majority of cells within the population at the peak of infection, HCV can induce variable cytopathology, and the surviving cells show fluctuating levels of viral replication and secretion of infectious virus over a 6-month period. For the convenience of discussion, we define the acute phase of infection as the time following primary virus infection, leading to a peak of extracellular-infectious-virus levels, followed by a period of cytopathology, leading to a trough of viral replication. The chronic phase of infection is defined as the events that transpire thereafter.

Enhancement of HCV infectivity during persistent infection. Although the levels of extracellular infectious virus and intracellular viral RNA fluctuate considerably during the chronic phase of Exp 1, the levels of extracellular infectious virus regularly returned to the initial day-18 peak while the intracellular RNA content did not. Furthermore, the frequency of NS5A-positive cells during the chronic phase was always below 50% (often below 1%), compared to nearly 100% at the peak of the acute phase. (Fig. 1A). These results suggest that either more virus particles are produced per intracellular RNA molecule or the secreted virus particles are more infectious. To investigate these two possibilities, we collected the extracellular virus from Exp 1 on days 18, 119, 155, and 183 posttransfection and examined their ability to expand in naïve Huh-7.5.1 cells after inoculation at an MOI of 0.002. As illustrated in Fig. 2A, the chronic-phase (days 119, 155, and 183) virus titers increased more rapidly than the acute-phase (day 18) virus titers (Fig. 2A). In keeping with these findings, the intracellular-HCV-RNA levels also increased more rapidly in the chronic-phase-virus-infected cells (data not shown). In addition, the chronic-phase viruses produced higher peak infectivity titers (10^5 to 10^6 FFU/ml) than the acute-phase viruses (1.6×10^4 FFU/ml). We repeated the infection kinetics assay by using

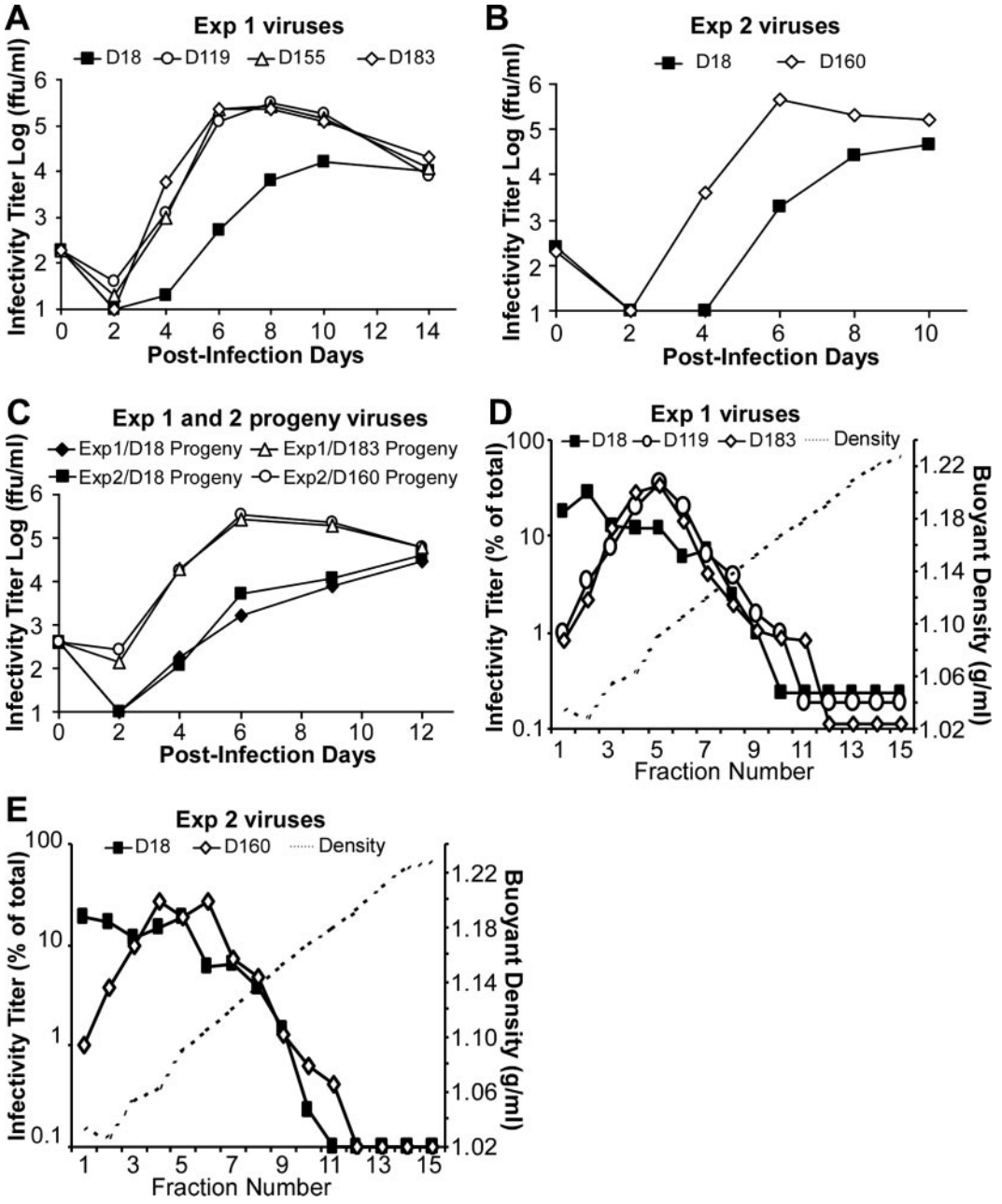

FIG. 2. Viral evolution during persistent infection. (A and B) Kinetics of viral production after infection with acute- and chronic-phase viruses. Huh-7.5.1 cells were inoculated at an MOI of 0.002, with viral supernatants collected on day 18, 119, 155, or 183 posttransfection in Exp 1 (A) or on day 18 or 160 posttransfection in Exp 2 (B). The supernatants were harvested at the indicated time points after infection and the infectivity titers determined. (C) Kinetics of viral production after infection with progeny of acute- and chronic-phase viruses. Huh-7.5.1 cells were inoculated at an MOI of 0.004 with progeny of day 18 and day 183 viruses (Exp 1) and day 18 and day 160 viruses (Exp 2). The supernatants were harvested at the indicated time points after infection and the infectivity titers determined. (D and E) Buoyant densities of acute- and chronic-phase viruses. The viruses collected at days 18, 119, and 183 posttransfection in Exp 1 (D) and the viruses collected at day 18 and day 160 posttransfection in Exp 2 (E) were analyzed in a 20 to 60% sucrose gradient. The infectivity titer for each fraction was determined, and the density of each fraction was determined by measuring the mass of a 100-μl aliquot of the fraction. The infectivity titer for each fraction is expressed as the percentage of the total titer for all fractions.

progeny of day 18 and day 183 viruses, both of which were collected on day 8 postinfection in the infection experiment described in the legend to Fig. 2A. As shown in Fig. 2C, the progeny of the day 183 virus expanded more rapidly and reached a higher titer than the progeny of day 18 virus, suggesting that the enhanced infectivity is likely due to changes in the genomes of chronic-phase viruses. This notion was further confirmed by transfecting chronic-phase-viral-RNA genomes into naïve Huh-7.5.1 cells and then monitoring the viral-expansion kinetics (Document S2 in the supplemental material).

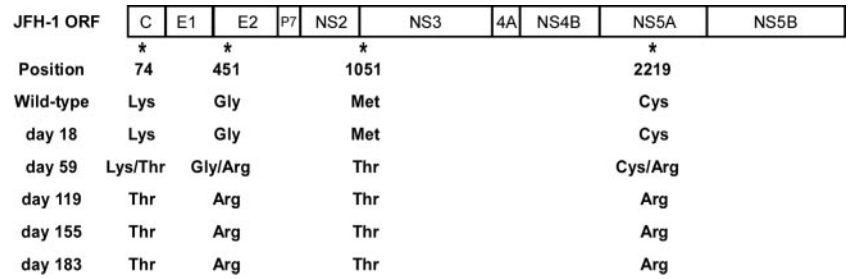

FIG. 3. Genetic mutations identified during persistent infection. A schematic diagram of the JFH-1 open reading frame is shown on the top. The numbers for the amino acid positions where mutations were identified in Exp 1 are marked with asterisks.

To determine whether the chronic-phase viruses from Exp 2 and Exp 3 also acquired enhanced infectivities, we inoculated naïve Huh-7.5.1 cells with viruses collected on days 18 and 160 posttransfection in Exp 2 and on days 26 and 99 posttransfection in Exp 3 and monitored the viral-expansion kinetics as described above. As shown in Fig. 2B, the day 160 virus from Exp 2 displayed more-rapid kinetics and reached a higher titer than the day 18 virus. Moreover, the enhanced infectivities of this virus could be passed to its progeny (Fig. 2C). In contrast, the kinetics and maximal titer displayed by the chronic-phase virus (day 99) from Exp 3 were comparable to those displayed by the acute-phase virus (day 26) in that experiment (data not shown).

The buoyant densities of viral particles change during persistent infection. To compare the biophysical properties of the viral particles produced during the acute and chronic phases of infection, we analyzed the buoyant densities of day 18 virus with those of day 119 and day 183 viruses from Exp 1 by sucrose density gradient ultracentrifugation analysis. As shown in Fig. 2D, the buoyant densities of the day 18 virus were distributed over a broad range (between 1.03 and 1.16 g/ml), whereas the lowest-density fractions of the day 119 and 183 viruses contained minimal infectivities, resulting in a rightward shift in the mean density of the virus. Importantly, progeny of chronic-phase viruses displayed a similar buoyant-density change (data not shown), suggesting that genetic changes in the chronic-phase viral genome are responsible for this phenotype. We also analyzed the buoyant densities of chronic-phase viruses in Exp 2 and Exp 3. As shown in Fig. 2E, chronic-phase virus (day 160) from Exp 2 displayed a similar density change, while the density profile for day 99 virus from Exp 3 was similar to that for the acute-phase virus (data not shown).

Identification of genetic mutations in chronic-phase virus. To identify the genetic changes that are responsible for the observed phenotypic changes in the chronic-phase viruses, we sequenced the RNA genomes of viruses collected on days 18, 59, 119, 155, and 183 posttransfection in Exp 1. There were no mutations in the day 18 virus, but mutations were identified in the chronic-phase viruses. As shown in Fig. 3, four mutations appeared in the day 59 virus (K74T in core, G451R in E2, M1051T in NS3, and C2219R in NS5A) and became fixed and maintained in viruses isolated on days 119, 155, and 183 posttransfection, implying that they were all present in the majority of viral genomes at those time points. The appearance of these mutations was associated with the appearance of enhanced infectivity and the changed density profiles.

To determine whether these mutations were responsible for the enhanced infectivities and altered densities of the chronic-phase virus, we engineered each mutation individually into the JFH-1 genome. The in vitro-transcribed recombinant JFH-1 RNA was electroporated into Huh-7.5.1 cells, and the ability of the resultant viruses to expand in naïve Huh-7.5.1 cells was examined. As shown in Fig. 4A, the G451R (E2) virus expanded more rapidly and reached higher titers than the wild type and other mutant viruses, suggesting that the G451R mutation in E2 is responsible for enhanced infectivity. We also noted that the G451R mutant virus displayed an accelerated cytopathic effect compared to the wild-type virus (data not shown). Furthermore, sucrose density analysis indicated that the buoyant densities of the G451R virus were similar to those of the chronic-phase viruses, while the densities of the other mutant viruses were similar to those of wild-type JFH-1 virus (Fig. 4A). These results suggest that the mutation in the viral-envelope glycoprotein E2 is primarily responsible for both the enhanced infectivities and the density changes seen in chronic-phase viruses.

The increased level of infectious virus obtained from chronically infected cultures may result from an increase in the absolute number of particles secreted or an increased proportion of infectious particles relative to noninfectious particles. To address this question, we compared the specific infectivities of mutant viruses and those of viruses collected from different phases of infection and determined the ratio of viral infectivity titer (FFU/ml) to HCV RNA (GE/ml) content. As shown in Fig. 4B, the chronic-phase (D183) and G451R (E2) viruses had higher specific-infectivity titers (1:294 and 1:312, respectively) than acute-phase and other single-point-mutant viruses (between 1:2,240 and 1:5,320), suggesting that particles released from long-term chronically infected cultures are more infectious, and the glycine-to-arginine substitution at position 451 in E2 appears to be responsible for the altered specific infectivities.

To illuminate the mechanism of action of the G451R mutation, we compared the infection of Huh-7.5.1 cells by the wild-type and G451 mutant viruses in the presence of increasing concentrations of CD81 antibody. As shown in Fig. 4C, although the CD81 antibody could block the infection by both the wild-type and the G451R mutant viruses, it appears that the infection by the mutant virus is less dependent upon the cell surface CD81 molecules than the infection by the wild-type virus, suggesting that the G451R mutation may confer a selective advantage to the mutant virus at the entry level.

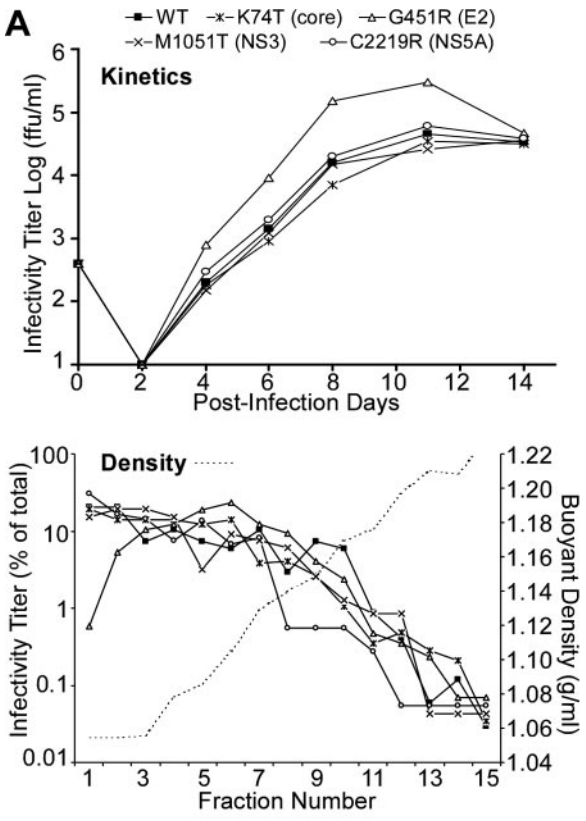

B

Virus	Maximal Titer (ffu/ml)	Specific infectivity (titer:RNA) (ffu:GE)
Exp 1 D18	4×10^4	1:2240
Exp 1 D183	2.6×10^5	1:294
K74T (core)	5.6×10^4	1:2303
G451R (E2)	3×10^5	1:312
M1051T (NS3)	8.6×10^4	1:5320
C2219R (NS5A)	7×10^4	1:3257

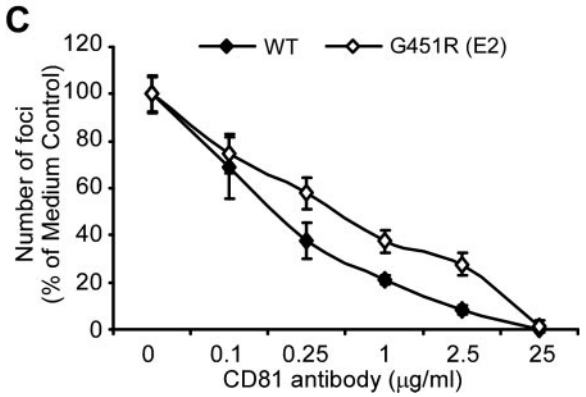

FIG. 4. The G451R mutation in E2 is responsible for the enhanced infectivities and altered buoyant densities of chronic-phase virus. (A) Infection kinetics and buoyant densities of mutant viruses. Top: Huh-7.5.1 cells were inoculated at an MOI of 0.004 with mutant JFH-1 viruses, and the supernatants were harvested at the indicated time points after infection and the infectivity titers determined. Bottom: mutant viruses were subjected to a 20 to 60% sucrose gradient, and the infectivity titer for each fraction was determined. The density of each fraction was determined by measuring the mass of a 100-μl aliquot of the fraction and is the average for four gradients. WT, wild type. (B) Specific-infectivity titers for acute- and chronic-phase virus (progeny of day 18 and 183 viruses in Exp 1) and mutant JFH-1 viruses. The wild-type and mutant viruses were prepared from the same experiment. Each specific-infectivity titer is the average for two measurements. (C) Blockade of HCV infection by CD81 antibody. The Huh-7.5.1 cells were pretreated with 0, 0.1, 0.25, 1, 2.5, and 25 μg/ml of CD81 antibody (clone 5A6) for 1 h and then infected with ~50 focus-forming units of the wild-type or G451R mutant viruses for 3 days. The infection was monitored by HCV immunofluorescence, and the numbers of HCV-positive foci were counted. Each result is expressed as a fraction of the number of foci observed in wells that received medium instead of anti-CD81. The error bars represent the standard deviations for four replicates.

Emergence of HCV-resistant cells during persistent infection. As shown in Fig. 1, the intracellular-HCV-RNA levels and frequency of NS5A-positive cells during the chronic phase of infection are lower than those seen at the peak of the acute phase, despite the increased infectivities of the chronic-phase viruses (Fig. 2). Indeed, as shown in Fig. S4A in the supplemental material, as few as 2% of the persistently infected cells were NS5A positive on day 85 posttransfection in Exp 1. Nonetheless, the virus produced by those cells was able to infect more than 60% of naïve Huh-7.5.1 cells within 3 days of inoculation (Fig. S4B in the supplemental material), raising the possibility that some cells within the persistently infected cell culture are resistant to HCV infection. To test this hypothesis, we inoculated persistently infected Huh-7.5.1 cells from Exp 2 with viruses collected from Exp 1. As shown in Fig. S5 in the supplemental material, although naïve Huh-7.5.1 cells were efficiently infected by HCV (more than 80% NS5A-positive cells on day 9 postinfection), the persistently infected cells appeared resistant to secondary infection.

One explanation for this resistance is that HCV is present within all cells of the persistently infected culture beneath the level of detection of NS5A immunofluorescence. In this case, secondary HCV infection could be inhibited by previously activated host antiviral mechanisms or by competition for host cell resources. To examine these possibilities, we isolated NS5A-negative cells from Exp 1 (on day 119), Exp 2 (on day 72), and Exp 3 (on day 160) by serial dilution and demonstrated the cells to be free of HCV RNA by RT-QPCR analysis ($<3 \times 10^{-5}$ GE per cell). These cells were named R1, R2, and R3 cells, respectively. To determine whether these HCV-negative cells could be infected by JFH-1, they were inoculated, along with parental Huh-7.5.1 and Huh-7/scr cells, with HCV (day 18 of Exp 2) at an MOI of 0.05. Cells were stained for NS5A protein 3 days later. As shown in Fig. 5A, 80% of Huh-7.5.1 (Fig. 5A, panel I) and 50% of Huh-7/scr (Fig. 5A, panel V) cells were NS5A positive, while 0.06% of R1 (Fig. 5A, panel II), 1% of R2 (Fig. 5A, panel III), and <0.01% of R3 (Fig. 5A, panel VI) cells were NS5A positive at this time point. In parallel experiments, we demonstrated that the R1, R2, and R3 cells were resistant to HCV from different sources, includ-

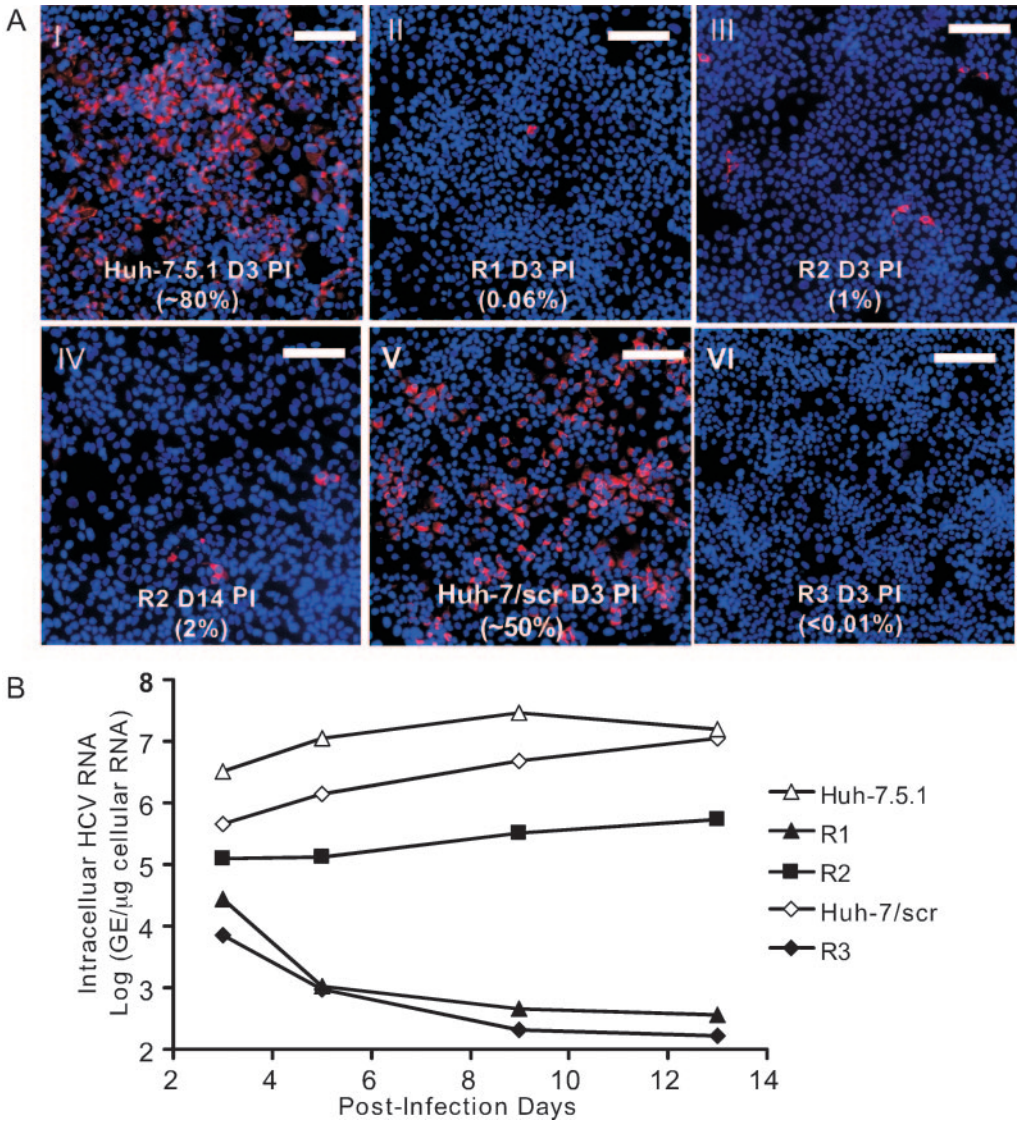

FIG. 5. The emergence of HCV-resistant cells during persistent infection. (A) NS5A staining of naïve Huh-7.5.1 (I), R1 (II), R2 (III), Huh-7/scr (V), and R3 (VI) cells that were infected with HCV at an MOI of 0.05 for 3 days and NS5A-staining of R2 (IV) cells that were infected with HCV at an MOI of 0.01 for 14 days. The estimated frequency for NS5A-positive cells is indicated on the bottom of each image. For all images, NS5A staining is in red (Alexa 555), and nuclei were stained with Hoechst (blue). The white scale bars represent 100 μM. (B) R1, R2, R3, and their parental Huh-7.5.1 and Huh-7/scr cells were infected with acute-phase HCV (day 18 in Exp 1) at an MOI of 0.01. The cells were harvested at the indicated time points after infection, and the intracellular-HCV-RNA levels were determined by RT-QPCR and normalized to cellular GAPDH levels.

ing day 18 (MOI, 0.05) and day 183 (MOI, 0.15) viruses from Exp 1; day 160 (MOI, 0.15) virus from Exp 2; and day 26 (MOI, 0.05) virus from Exp 3 (data not shown).

To demonstrate that the low frequency of NS5A-postive cells on day 3 postinfection was not merely a reflection of delayed infection kinetics in these cells, we monitored the intracellular-HCV-RNA levels for 13 days following infection. As shown in Fig. 5B, the intracellular-HCV-RNA levels in R1 and R3 cells decreased to 10^2 to 10^3 GE per μg cellular RNA on day 13 postinfection, at which point no NS5A-positive cells were detected by immunofluorescence (data not shown). In contrast, R2 cells appeared more susceptible to HCV infection than R1 and R3 cells, but JFH-1 infection was impaired relative to parental Huh-7.5.1 cells (Fig. 5B). Importantly, the intracellular-HCV-RNA levels in R2 cells failed to increase significantly even by 13 days postinfection, and the frequency of NS5A-postive cells was approximately 2% by 14 days postinfection (Fig. 5A, panel IV). Taken together, these results suggest that host cells evolve during persistent infection to become resistant to HCV infection.

Loss of cellular CD81 expression during persistent infection. To elucidate the mechanism(s) for resistance to HCV infection, we compared the cell surface expression of the viral coreceptor CD81 on parental Huh-7 and Huh-7.5.1 cells with that on R1, R2, and R3 cells by flow cytometry. CD81 cell surface expression levels on R3 and R1 cells were greatly

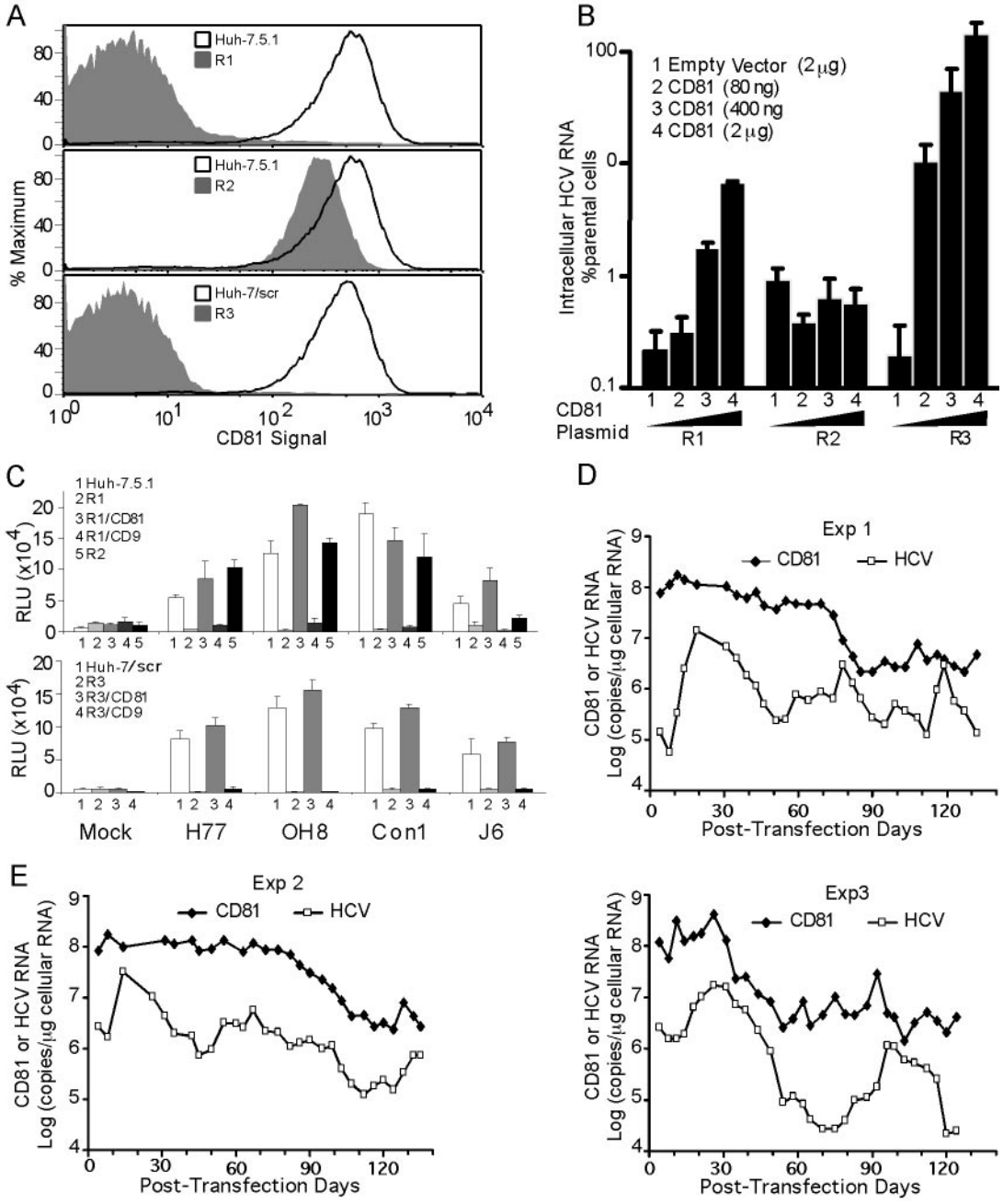

FIG. 6. Loss of CD81 expression in persistently infected cells. (A) CD81 cell surface staining of R1, R2, R3, and their parental Huh-7.5.1 and Huh-7/scr cells. The cells were stained with a mouse anti-human CD81 antibody followed by a phycoerythrin-conjugated secondary antibody. (B) Intracellular-HCV-RNA levels in the CD81-transfected R1, R2, and R3 cells 3 days after infection. Cells were transfected with 80 ng, 400 ng, and 2 μg of the CD81 expression plasmid (pEE6-hCD81) or 2 μg pCDNA3 plasmid. At 48 h posttransfection, the cells were infected with HCV (day 18 of Exp 1) at an MOI of 0.1. The intracellular-HCV-RNA levels were analyzed by quantitative RT-PCR, normalized to the cellular GAPDH levels, and expressed as the percentages of the intracellular-HCV-RNA levels in the corresponding parental cells. The error bars represent the standard deviations for three measurements. (C) Infection of parental Huh-7.5.1, Huh-7/scr, and resistant R1, R2, and R3 cells, before and after transduction with lentiviral vectors expressing CD81 and the related tetraspanin CD9, with HCVpp bearing H77, OH8, Con1, and J6 glycoproteins. Results are expressed as numbers of relative light units (RLU) normalized based on a control MLV pseudotyped-retroviral-particle infection. (D, E, and F) CD81 mRNA levels during the entire course of persistent infection in Exp 1 (D), Exp 2 (E), and Exp 3 (F). CD81 mRNA levels were measured by RT-QPCR and normalized to cellular GAPDH levels.

reduced compared to those on their respective parental populations (Fig. 6A and Fig. S7 in the supplemental material), and these observations were confirmed at the CD81 mRNA level by RT-QPCR (data not shown). In contrast, R2 cells showed relatively normal CD81 expression levels, although the intensity of CD81 staining was slightly reduced compared to that for the parental cells (Fig. 6A). We also examined cell surface expression levels of scavenger receptor class B type I

(SR-BI), an additional viral coreceptor (3, 23, 24). SR-B1 was expressed at similar levels in the resistant and parental cells (data not shown).

To confirm that the reduced susceptibilities of R1 and R3 cells to JFH-1 infection is due to the lack of CD81 expression, we transfected increasing amounts of a CD81 expression vector (12) into R1, R2, and R3 cells. On day 2 posttransfection, we determined CD81 cell surface expression levels by flow cytometry and infected transfected cells with JFH-1 at an MOI of 0.1. As shown in Fig. S6 in the supplemental material, transfection of CD81-expressing plasmids restored CD81 cell surface expression in R1 and R3 cells in a dose-dependent manner, while CD81 cell surface expression levels in R2 cells remained unchanged. More importantly, R3 cells transfected with the CD81 plasmid could be efficiently infected by JFH-1, with maximal CD81 expression restoring the infection to levels seen in the parental Huh-7/scr cells (Fig. 6B). CD81 expression in R1 cells rescued JFH-1 infection, albeit less efficiently than that in R3 cells. In contrast, the susceptibility of R2 cells to JFH-1 infection remained unchanged after CD81 transfection, suggesting that the defect(s) in R2 cells is independent of CD81 expression.

To confirm that the block to infection of R1 and R3 cells was at the level of viral entry, we infected these cells with pseudotyped lentiviruses bearing diverse HCV envelope glycoproteins E1 and E2 (HCVpp) (H77, OH8, Con1, and J6). As shown in Fig. 6C, the R1 and R3 cells were resistant to HCVpp infection while the parental Huh-7.5.1 and Huh-7/scr cells and the R2 cells were susceptible to infection. Transduction of cells to express CD81, but not CD9, a negative control, restored CD81 cell surface expression in R1 and R3 cells (Fig. S7 in the supplemental material) and their ability to support HCVpp infection (Fig. 6C). Collectively, these results illustrate that the resistance to HCV infection observed in R1 and R3 cells is due to the absence of CD81 expression in these cells.

To determine when the CD81-negative cells emerged during the persistent infection, we analyzed CD81 mRNA levels throughout the course of infection in Exp 1, Exp 2, and Exp 3 (Fig. 6D, E, and F). As expected, we observed a significant decrease in CD81 mRNA levels during persistent infection in Exp 1 and Exp 3 prior to the time when the R1 (day 119) and R3 (day 160) cells were derived, respectively. CD81 mRNA levels decreased between days 69 and 85 posttransfection in Exp 1 and between days 26 and 54 posttransfection in Exp 3. Interestingly, CD81 expression levels also decreased between days 77 and 116 posttransfection in Exp 2, but this decrease occurred after the CD81-positive R2 cells were isolated (day 72).

Inhibition of HCV RNA replication during persistent infection. The aforementioned results demonstrate that R2 cells are relatively resistant to HCV infection despite expressing CD81 and supporting HCVpp entry. In addition, CD81 transfection of R1 cells only partially rescued infection by JFH-1 but could fully restore HCVpp entry (Fig. 6B and C). These results suggest that R1 and R2 cells have an additional defect(s) downstream from viral entry. To test this possibility, we examined the abilities of these cells to support HCV replicon replication. As shown in Fig. 7, R3 cells were able to support HCV replicon replication as efficiently as naïve Huh-7 cells, whereas the abilities of R1 and R2 cells to support replicon replication were greatly reduced, suggesting that inefficient HCV RNA replication in R1 and R2 cells likely contributed to the resistance to JFH-1 infection.

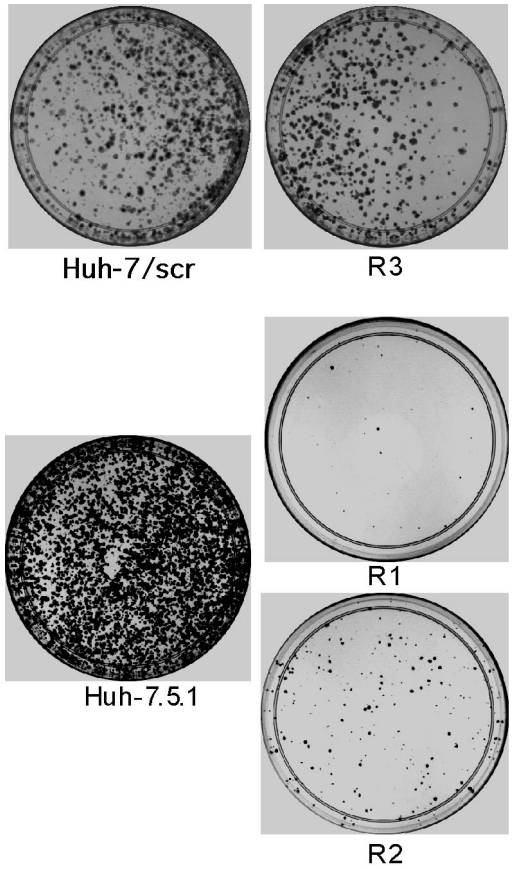

FIG. 7. R1 and R2 cells do not support HCV replicon replication efficiently. One microgram of genotype 1b subgenomic replicon (S1179I) was electroporated into 4×10^6 Huh-7/scr, R3, Huh-7.5.1, R1, and R2 cells. One-third of the cells were plated on a 10-cm dish and subjected to 300 μg/ml G418 selection for 3 weeks. The colonies were fixed and stained with crystal violet.

To assess whether the resistance to HCV infection observed in R1, R2, and R3 cells extended to other viruses, we inoculated them and the parental Huh-7.5.1 and Huh-7/scr cells with vesicular stomatitis virus. Our results indicated that the HCV-resistant cells were as susceptible to vesicular stomatitis virus infection as their parental cell lines (data not shown).

DISCUSSION

Using a recently established system to propagate infectious HCV based on a genotype 2a JFH-1 strain of HCV (25, 31), we report that JFH-1 can persistently infect Huh-7/scr and Huh-7.5.1 cells for periods of 6 months or more. The system is characterized by a variable cytopathic effect at the peak of acute infection and by fluctuating levels of extracellular infectious virus, intracellular HCV RNA, and HCV-infected cells during the persistent phase of infection. Interestingly, both the virus and the host cell evolve during persistent infection, with the virus acquiring increased specific infectivity and the host cells becoming resistant to HCV infection.

HCV infection can be cytopathic in vitro. HCV has long been regarded as a noncytopathic virus. The destruction of hepatocytes during HCV-associated hepatitis is believed to be the result of cytotoxic-T-cell-mediated clearance of HCV-infected hepatocytes. Interestingly, we observed that, in the absence of an adaptive immune response, JFH-1 can induce cytopathic effects in Huh-7.5.1 cells and, to a lesser degree, in the Huh-7 cells. The molecular basis for this observation is not clear; however, the cytopathic potential of the JFH-1 clone may reflect the fact that it is based on the consensus sequence of a genotype 2a virus that was isolated from a patient with acute fulminant hepatitis, an extremely rare event. It is worth noting that infection of chimpanzees with JFH-1 or J6/JFH failed to induce fulminant hepatitis; however, the levels of replication observed in the infected animals were low (17, 25). Since the magnitude of the cytopathic effect is greater in the RIG-I-deficient Huh-7.5.1 cells than in Huh-7/scr cells, cellular factors may also contribute to the cytopathic effect. Additional studies will be necessary to understand the pathophysiological basis for these different outcomes.

Virus evolution during persistent infection. Mutation of glycine to arginine at amino acid (a.a.) 451 in E2 is primarily responsible for the more rapid viral-expansion kinetics, higher infectious titers, increased specific infectivities, and buoyant-density changes observed in viruses that evolved in Exp 1. The increased specific infectivities of the E2 mutant virus suggests that this mutation allows more-efficient production of infectious viral particles. The infection by the G451R mutant virus appears to be less dependent upon the CD81 molecules on the cell surface than that by the wild-type virus, which gives the virus a selective advantage during the late period of persistent infection when the CD81-deficient cells emerge. The glycine at position 451 is located between hypervariable region 1 (a.a. 384 to 410) and hypervariable region 2 (a.a. 474 to 482) within the N terminus of E2 (28), a region that has been reported to modulate the accessibility of the CD81 binding site (22). This residue appears to be conserved, since BLAST analysis of 502 HCV sequences in the NCBI database yielded only one sequence (BAA03375) encoding an arginine at this position as seen with the chronic-phase virus from Exp 1. It will be interesting to observe the kinetics, magnitude, and severity of infection of a G451R mutant virus in vivo.

In addition to the change in E2, mutations in core (K74T), NS3 (M1051T), and NS5A (C2219R) were selected for chronic-phase viruses in Exp 1. Recombinant viruses containing these mutations were produced by transfecting in vitro-transcribed RNA into Huh-7.5.1 cells, suggesting that the wild-type amino acids at these positions are not essential for virus viability. Interestingly, we did not detect significant differences in the viral-expansion kinetics and buoyant-density profiles between the mutant and wild-type viruses. Given that these mutations were selected during persistent infection, they may favor HCV survival and/or expansion in ways that remain to be determined.

Although chronic-phase virus (day 160) from Exp 2 displayed more-rapid expansion kinetics and altered buoyant densities, it does not contain the G451R mutation. Nonetheless, other mutations were observed in this isolate, including V22A and K74Q in core and V388P, I414T, and L644I in E2. It is possible that one or more of these mutations could be responsible for the phenotype of the day 160 virus, and this hypothesis is currently under investigation. Interestingly, the chronic-phase virus from Exp 3 did not show enhanced infectivities or changes in buoyant density as observed in viruses from Exp 1 and Exp 2. One possible explanation is that the intracellular-HCV-RNA levels are lower in the persistently infected Huh-7/scr cells (Exp 3) than in Huh-7.5.1 cells (Exp 1 and Exp 2), thereby reducing opportunities for random mutations.

Interestingly, we observed a change in the buoyant densities of the chronic-phase viruses from Exp 1 and Exp 2. Such a density change for HCV is not unusual in vivo. It has been reported that the densities of HCV isolated from chronic hepatitis patients are higher than those of acute virus (21, 26), although it was suggested that the higher densities reflect the presence of virus-bound antibodies. Based on our current results, we speculate that the change in viral density occurring during persistent infection in cell culture reflects changes in the composition of virus-associated cellular proteins or the lipid composition of the viral envelope, likely due to the mutation in E2. Further investigation will be necessary to test these hypotheses.

Host evolution during persistent infection. Another exciting aspect of these results is the rapid emergence of cells that are resistant to HCV infection and dominate the persistently infected cell culture. HCV-free cells derived from three independent persistent infections displayed resistance to JFH-1 infection. We do not know whether small numbers of resistant cells were present in the parental Huh-7/scr and Huh-7.5.1 cell lines or whether they emerged during HCV infection. In either scenario, however, selective forces likely imposed by the virus were responsible for the outgrowth and dominance of the resistant cells. More experiments will be needed to identify the basis for selection. The minor frequency of cells that support HCV replication in the resistant cell lines may reflect the heterogeneous nature of these cells, since the resistant cell lines were not isolated from a single clone, or various CD81 expression levels, some of which are above a threshold level required for HCV infection (A. Jennings and J. A. McKeating, unpublished data).

Importantly, different mechanisms are responsible for resistance to HCV infection in the three resistant cell lines obtained. R3 cells lack CD81 cell surface expression, which explains their inability to support JFH-1 infection and HCVpp entry. This defect can be fully complemented by CD81 transfection or transduction, indicating that the lack of CD81 expression in R3 cells forms the basis for their resistance to JFH-1 infection. In contrast, R2 cells express CD81 at a level comparable to those for the parental cells and support HCVpp entry but fail to support efficient JFH-1 infection, suggesting a defect downstream of viral entry, most likely at the level of viral-RNA replication. Interestingly, R1 cells display defects in both HCVpp entry and HCV RNA replication. Both defects may be necessary for efficient curing of viral infection since initiation and spread of viral infection are efficiently inhibited by blocking viral entry, while inhibition of viral-RNA replication is better suited for purging virus from existing infected cells. Further experiments are needed to identify the molecular basis of the defect(s) in HCV RNA replication in R1 and R2 cells.

Perspectives. The current observations illustrate several general principles that may be relevant for the pathophysiology of HCV and other persistent RNA viral infections. For example, the evolution of cells that are resistant to HCV infection in vitro raises the possibility that similar events may occur within the persistently infected liver. Indeed, although it is difficult to quantify HCV-infected cells in vivo, Bigger and colleagues, using quantitative HCV RNA analysis of liver RNA from acutely (5) and chronically (6) HCV-infected chimpanzees, estimated that between 0.1% and 30% of hepatocytes may be infected at any point in time and that the extents of infection may be limited by the relative magnitudes of the innate immune responses elicited in different animals. While we agree with this hypothesis, the results presented herein suggest that other factors may also be operative. For example, hepatocytes in the liver are a heterogeneous population of cells (13a) that could display differential susceptibilities to HCV infection. As a result, the constitutive resistance of a subset of hepatocytes to HCV infection, coupled with immune elimination of HCV-infected hepatocytes, may select for the repopulation of the liver with resistant cells during persistent infection. Similarly, viral variants with increased specific infectivities and relative levels of fitness for the environment of the persistently infected liver may evolve. Of course, we would expect the time scale of events in vivo to be much slower (requiring years, perhaps decades) than that of events observed in vitro (occurring in weeks) because of the differences in hepatocyte turnover rates under in vivo and in vitro conditions. Indeed, these events occur at a much slower pace in a new in vitro HCV infection model that we have recently developed using dimethyl sulfoxide-treated Huh-7/scr cells that are more highly differentiated than the rapidly dividing Huh-7/scr cells used in the current experiments and display growth arrest when becoming confluent (22a). Nonetheless, the principles illustrated in our in vitro experiments may provide new insights into the pathophysiology of persistent HCV infection in vivo where hepatocyte death and cell division are driven by the cytotoxic-T-cell response (9). Future experiments to extend these observations to other viral strains and target cells, particularly primary human hepatocytes, are clearly warranted. Finally, these results are consistent with reports that similar events of virus and host cell coevolution may contribute to the pathophysiology of persistent reovirus (1, 11), rotavirus (19), coronavirus (8), and foot-and-mouth disease virus (10) infections, illustrating the general principle of coevolutionary selection and emphasizing its biological and clinical importance.

ACKNOWLEDGMENTS

We thank Takaji Wakita (Tokyo Metropolitan Institute for Neuroscience) for providing the JFH-1 cDNA; Jens Bukh and Robert Purcell (National Institutes of Health) for providing the protocols of HCV genomic RNA sequencing; Michael Houghton (Chiron Corp.) for providing anti-NS5A antibodies; Christina Whitten, Bryan Boyd, Angie Eustaquio, Alana Althage, Susan Uprichard, and Shinichi Asabe for technical help; and Holly Maier for help in editing the manuscript.

This study was supported by NIH grant CA108304 to F.V.C. and AI50798 to J.A.M.

This paper is manuscript number 18186-MEM from The Scripps Research Institute.

We declare no conflict of interest.

REFERENCES

1. **Ahmed, R., W. M. Canning, R. S. Kauffman, A. H. Sharpe, J. V. Hallum, and B. N. Fields.** 1981. Role of the host cell in persistent viral infection: coevolution of L cells and reovoirus during persistent infection. Cell **25:**325–332.
2. **Bartenschlager, R., and V. Lohmann.** 2000. Replication of hepatitis C virus. J. Gen. Virol. **81:**1631–1648.
3. **Bartosch, B., A. Vitelli, C. Granier, C. Goujon, J. Dubuisson, S. Pascale, E. Scarselli, R. Cortese, A. Nicosia, and F. L. Cosset.** 2003. Cell entry of hepatitis C virus requires a set of co-receptors that include the CD81 tetraspanin and the SR-B1 scavenger receptor. J. Biol. Chem. **278:**41624–41630.
4. Reference deleted.
5. **Bigger, C. B., K. M. Brasky, and R. E. Lanford.** 2001. DNA microarray analysis of chimpanzee liver during acute resolving hepatitis C virus infection. J. Virol. **75:**7059–7066.
6. **Bigger, C. B., B. Guerra, K. M. Brasky, G. Hubbard, M. R. Beard, B. A. Luxon, S. M. Lemon, and R. E. Lanford.** 2004. Intrahepatic gene expression during chronic hepatitis C virus infection in chimpanzees. J. Virol. **78:**13779–13792.
7. **Blight, K. J., A. A. Kolykhalov, and C. M. Rice.** 2000. Efficient initiation of HCV RNA replication in cell culture. Science **290:**1972–1975.
8. **Chen, W., and R. S. Baric.** 1996. Molecular anatomy of mouse hepatitis virus persistence: coevolution of increased host cell resistance and virus virulence. J. Virol. **70:**3947–3960.
9. **Chisari, F. V.** 1997. Cytotoxic T cells and viral hepatitis. J. Clin. Investig. **99:**1472–1477.
10. **de la Torre, J. C., E. Martinez-Salas, J. Diez, A. Villaverde, F. Gebauer, E. Rocha, M. Davila, and E. Domingo.** 1988. Coevolution of cells and viruses in a persistent infection of foot-and-mouth disease virus in cell culture. J. Virol. **62:**2050–2058.
11. **Dermody, T. S., M. L. Nibert, J. D. Wetzel, X. Tong, and B. N. Fields.** 1993. Cells and viruses with mutations affecting viral entry are selected during persistent infections of L cells with mammalian reoviruses. J. Virol. **67:**2055–2063.
12. **Flint, M., C. Maidens, L. D. Loomis-Price, C. Shotton, J. Dubuisson, P. Monk, A. Higginbottom, S. Levy, and J. A. McKeating.** 1999. Characterization of hepatitis C virus E2 glycoprotein interaction with a putative cellular receptor, CD81. J. Virol. **73:**6235–6244.
13. **Hsu, M., J. Zhang, M. Flint, C. Logvinoff, C. Cheng-Mayer, C. M. Rice, and J. A. McKeating.** 2003. Hepatitis C virus glycoproteins mediate pH-dependent cell entry of pseudotyped retroviral particles. Proc. Natl. Acad. Sci. USA **100:**7271–7276.

13a. **Jungermann, K., and N. Katz.** 1989. Functional specialization of different hepatocyte populations. Physiol. Rev. **69:**708–764.

14. **Kato, T., T. Date, M. Miyamoto, A. Furusaka, K. Tokushige, M. Mizokami, and T. Wakita.** 2003. Efficient replication of the genotype 2a hepatitis C virus subgenomic replicon. Gastroenterology **125:**1808–1817.
15. **Lauer, G. M., and B. D. Walker.** 2001. Hepatitis C virus infection. N. Engl. J. Med. **345:**41–52.
16. **Lindenbach, B. D., M. J. Evans, A. J. Syder, B. Wolk, T. L. Tellinghuisen, C. C. Liu, T. Maruyama, R. O. Hynes, D. R. Burton, J. A. McKeating, and C. M. Rice.** 2005. Complete replication of hepatitis C virus in cell culture. Science **309:**623–626.
17. **Lindenbach, B. D., P. Meuleman, A. Ploss, T. Vanwolleghem, A. J. Syder, J. A. McKeating, R. E. Lanford, S. M. Feinstone, M. E. Major, G. Leroux-Roels, and C. M. Rice.** 2006. Cell culture-grown hepatitis C virus is infectious in vivo and can be recultured in vitro. Proc. Natl. Acad. Sci. USA **103:**3500–3501.
18. **McKeating, J. A., L. Q. Zhang, C. Logvinoff, M. Flint, J. Zhang, J. Yu, D. Butera, D. D. Ho, L. B. Dustin, C. M. Rice, and P. Balfe.** 2004. Diverse hepatitis C virus glycoproteins mediate viral infection in a CD81-dependent manner. J. Virol. **78:**8496–8505.
19. **Mrukowicz, J. Z., J. D. Wetzel, M. I. Goral, A. B. Fogo, P. F. Wright, and T. S. Dermody.** 1998. Viruses and cells with mutations affecting viral entry are selected during persistent rotavirus infections of MA104 cells. J. Virol. **72:**3088–3097.
20. **Pietschmann, T., A. Kaul, G. Koutsoudakis, A. Shavinskaya, S. Kallis, E. Steinmann, K. Abid, F. Negro, M. Dreux, F. L. Cosset, and R. Bartenschlager.** 2006. Construction and characterization of infectious intragenotypic and intergenotypic hepatitis C virus chimeras. Proc. Natl. Acad. Sci. USA **103:**7408–7413.
21. **Pumeechockchai, W., D. Bevitt, K. Agarwal, T. Petropoulou, B. C. Langer, B. Belohradsky, M. F. Bassendine, and G. L. Toms.** 2002. Hepatitis C virus particles of different density in the blood of chronically infected immunocompetent and immunodeficient patients: implications for virus clearance by antibody. J. Med. Virol. **68:**335–342.
22. **Roccasecca, R., H. Ansuini, A. Vitelli, A. Meola, E. Scarselli, S. Acali, M. Pezzanera, B. B. Ercole, J. McKeating, A. Yagnik, A. Lahm, A. Tramontano, R. Cortese, and A. Nicosia.** 2003. Binding of the hepatitis C virus E2 glycoprotein to CD81 is strain specific and is modulated by a complex interplay between hypervariable regions 1 and 2. J. Virol. **77:**1856–1867.

22a. **Sainz, B., Jr., and F. V. Chisari.** 2006. Production of infectious hepatitis C

virus by Well-differentiated, growth-arrested human hepatoma-derived cells. J. Virol. **80:**10253–10257.

23. **Scarselli, E., H. Ansuini, R. Cerino, R. M. Roccasecca, S. Acali, G. Filocamo, C. Traboni, A. Nicosia, R. Cortese, and A. Vitelli.** 2002. The human scavenger receptor class B type I is a novel candidate receptor for the hepatitis C virus. EMBO J. **21:**5017–5025.
24. **von Hahn, T., B. D. Lindenbach, A. Boullier, O. Quehenberger, M. Paulson, C. M. Rice, and J. A. McKeating.** 2006. Oxidized low-density lipoprotein inhibits hepatitis C virus cell entry in human hepatoma cells. Hepatology **43:**932–942.
25. **Wakita, T., T. Pietschmann, T. Kato, T. Date, M. Miyamoto, Z. Zhao, K. Murthy, A. Habermann, H. G. Krausslich, M. Mizokami, R. Bartenschlager, and T. J. Liang.** 2005. Production of infectious hepatitis C virus in tissue culture from a cloned viral genome. Nat. Med. **11:**791–796.
26. **Watson, J. P., D. J. Bevitt, G. P. Spickett, G. L. Toms, and M. F. Bassendine.** 1996. Hepatitis C virus density heterogeneity and viral titre in acute and chronic infection: a comparison of immunodeficient and immunocompetent patients. J. Hepatol. **25:**599–607.
27. **Wieland, S. F., L. G. Guidotti, and F. V. Chisari.** 2000. Intrahepatic induction of alpha/beta interferon eliminates viral RNA-containing capsids in hepatitis B virus transgenic mice. J. Virol. **74:**4165–4173.
28. **Yagnik, A. T., A. Lahm, A. Meola, R. M. Roccasecca, B. B. Ercole, A. Nicosia, and A. Tramontano.** 2000. A model for the hepatitis C virus envelope glycoprotein E2. Proteins **40:**355–366.
29. **Yi, M., A. Rodrigo, R. A. Villanueva, D. L. Thomas, T. Wakita, and S. M. Lemon.** 2006. Production of infectious genotype 1a hepatitis C virus (Hutchinson strain) in cultured human hepatoma cells. Proc. Natl. Acad. Sci. USA **103:**2310–2315.
30. **Zhang, J., G. Randall, A. Higginbottom, P. Monk, C. M. Rice, and J. A. McKeating.** 2004. CD81 is required for hepatitis C virus glycoprotein-mediated viral infection. J. Virol. **78:**1448–1455.
31. **Zhong, J., P. Gastaminza, G. Cheng, S. Kapadia, T. Kato, D. R. Burton, S. F. Wieland, S. L. Uprichard, T. Wakita, and F. V. Chisari.** 2005. Robust hepatitis C virus infection in vitro. Proc. Natl. Acad. Sci. USA **102:**9294–9299.